Supporting Information

A series of novel Cu-based MOFs: syntheses, structural diversity, catalytic properties and mimic peroxidase activity for colorimetric detection of H_2O_2

Juan Chai,‡[a] Luohao Yuan,‡[ac] Shiwei Wang,[a] Tong Li,[a] Mingxue Wu,[b] Zhiwei Huang,[a] Hongfeng Yin*[a]

[a]Ningbo Institute of Materials Technology and Engineering, Chinese Academy of Sciences, 1219 Zhongguan West Road, Ningbo, Zhejiang 315201, P. R. China

E-mail: yinhf@nimte.ac.cn

[b]School of Chemistry and Chemical Engineering, Qingdao University, Qingdao 266071, Shandong, P. R. China

[c]Institute of Industrial Catalysis, College of Chemical Engineering, State Key Laboratory Breeding Base of Green-Chemical Synthesis Technology, Zhejiang University of Technology, Hangzhou, 310032, China.

Supporting Information

Table of Contents

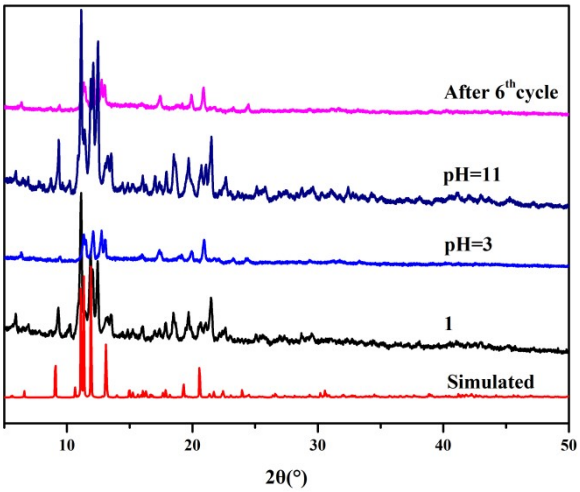

Fig .S1 Powder X-ray diffraction patterns of MOF **1**.

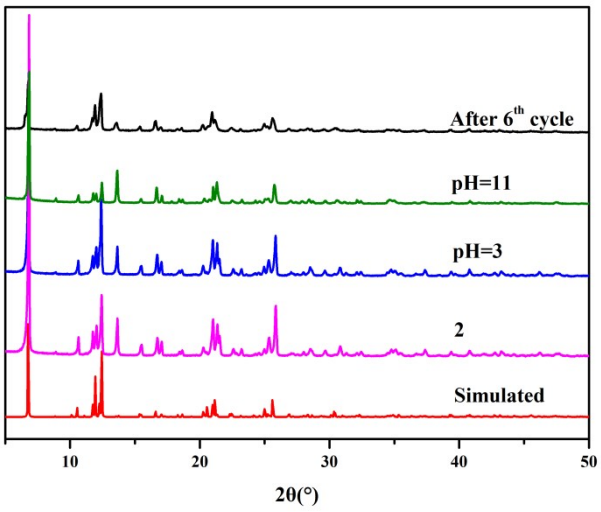

Fig. S2 Powder X-ray diffraction patterns of MOF **2**.

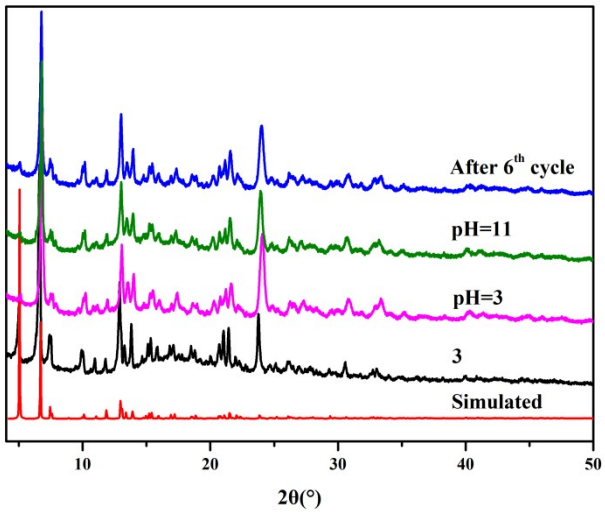

Fig. S3 Powder X-ray diffraction patterns of MOF **3**.

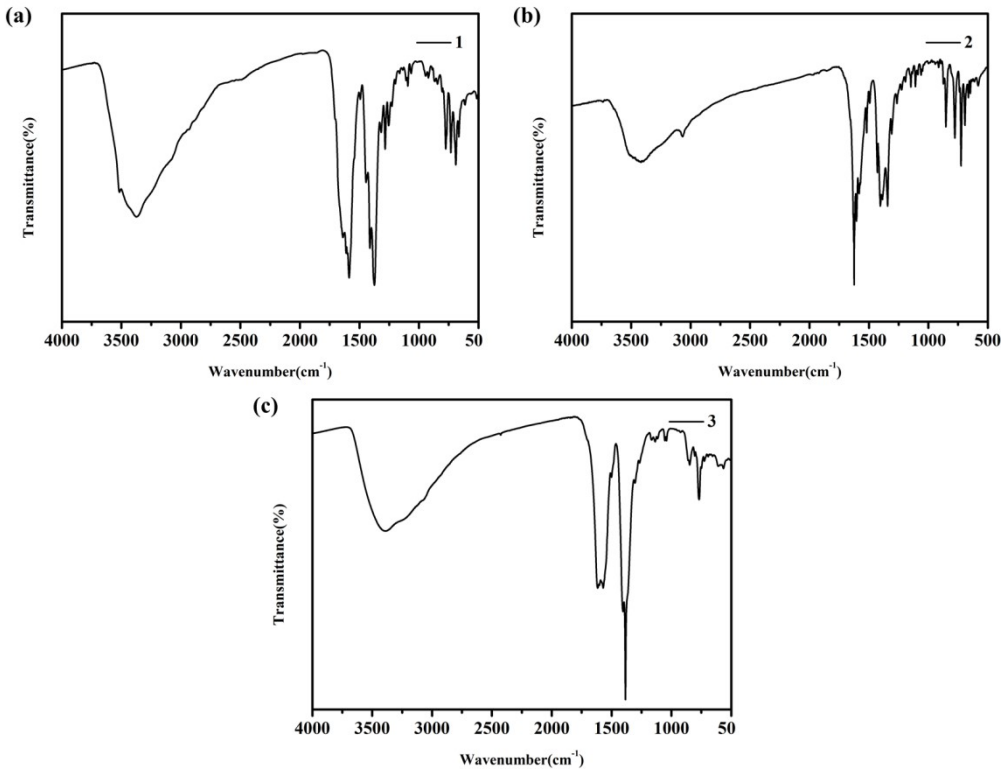

Fig. S4 FT-IR spectra of MOF **1** (a), MOF **2** (b) and MOF **3** (c).

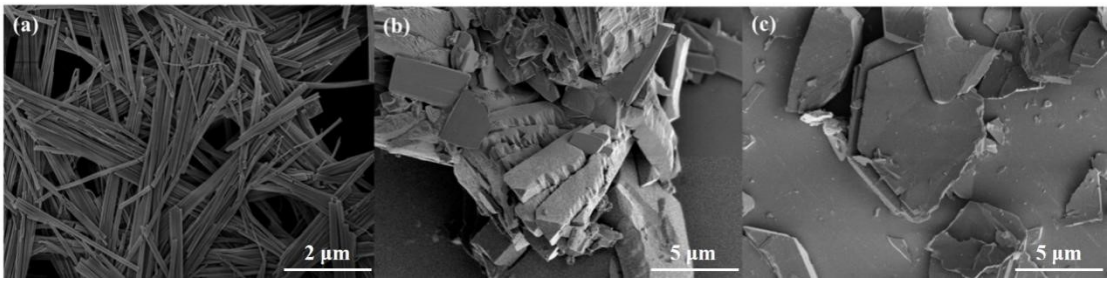

Fig. S5 SEM images of MOF **1** (a), MOF **2** (b) and MOF **3** (c).

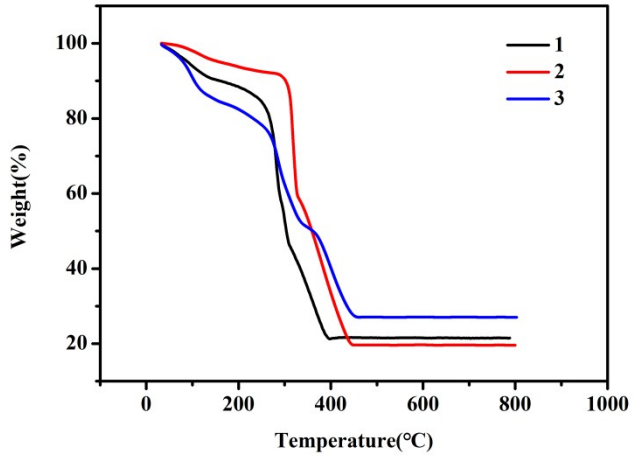

Fig. S6 TGA curves of MOFs **1-3** measured in air atmosphere.

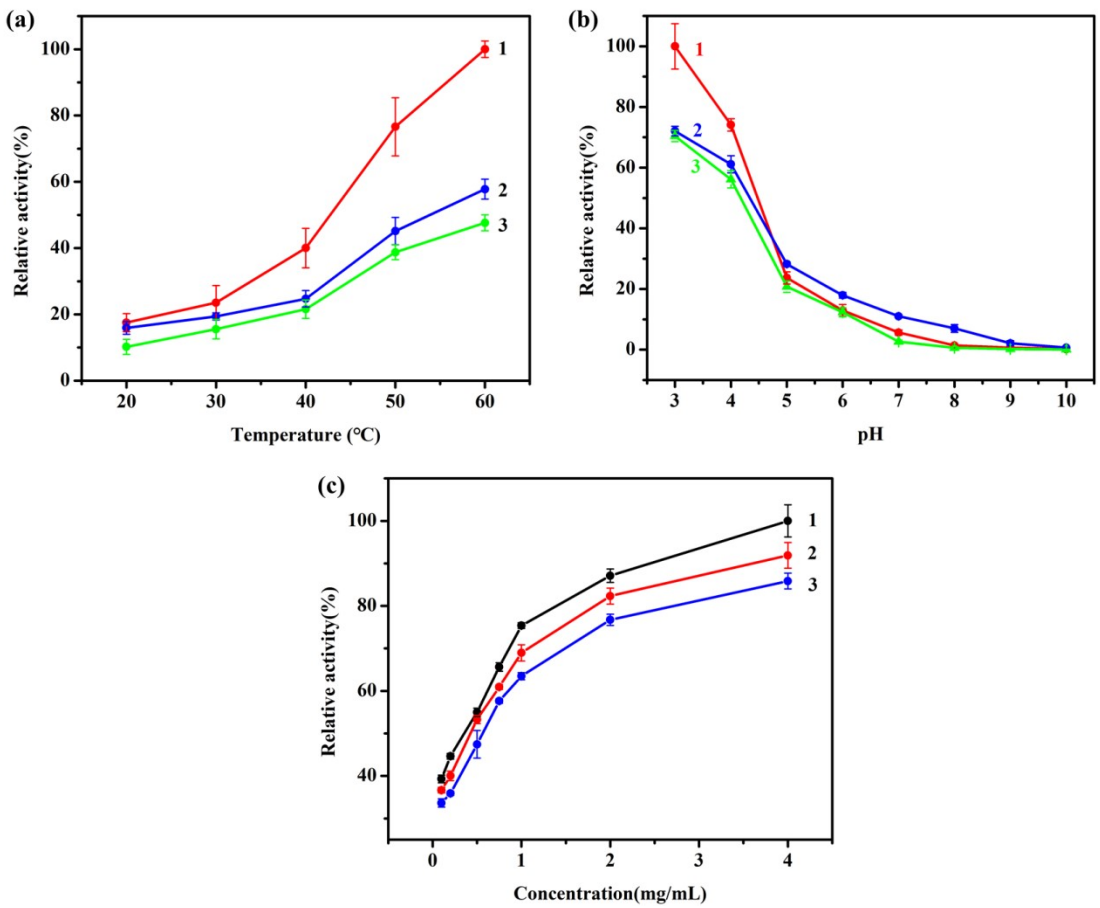

Fig. S7 Relative peroxidase activity of MOFs **1-3** at different temperatures (a), pH values (b) and concentrations of MOFs (c).

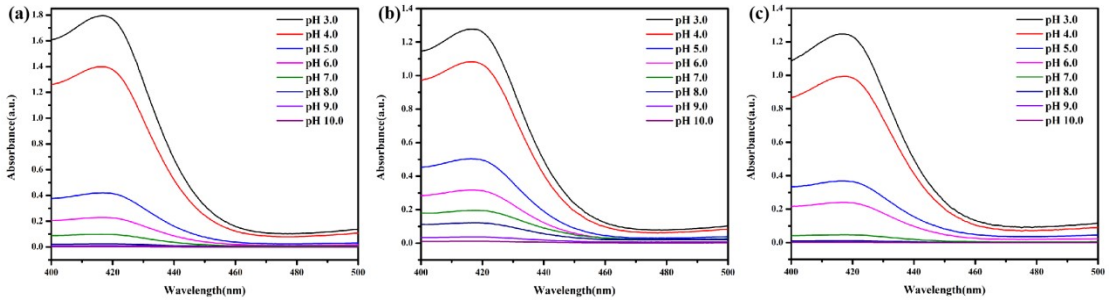

Fig. S8 UV-vis absorbance spectra at different pH values for **1** (a), **2** (b), **3** (c).

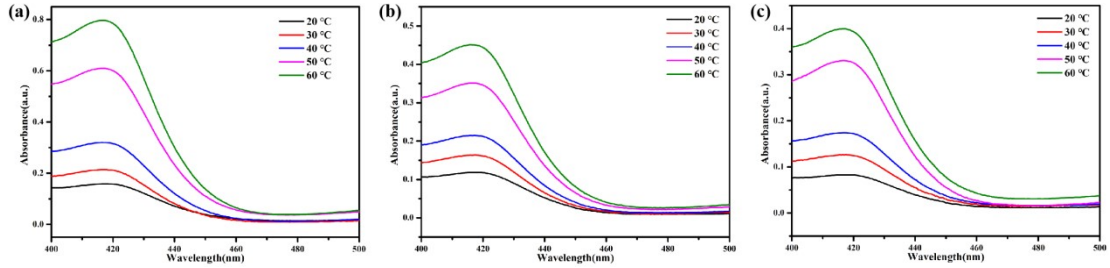

Fig. S9 UV-vis absorbance spectra at different temperature for **1** (a), **2** (b), **3** (c).

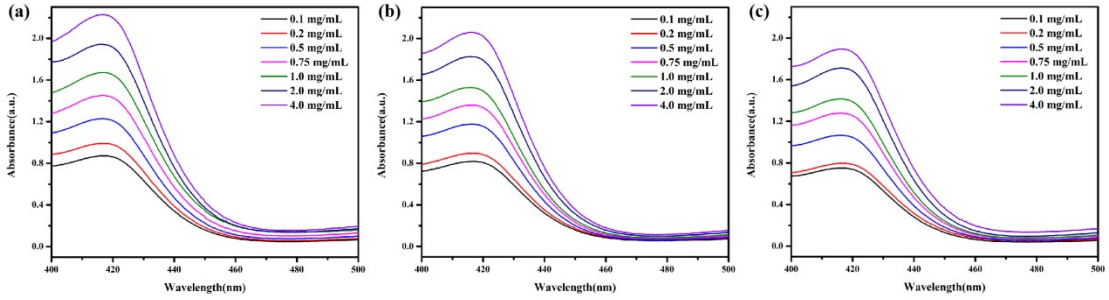

Fig. S10 UV-vis absorbance spectra at different concentrations of MOFs for **1** (a), **2** (b), **3** (c).

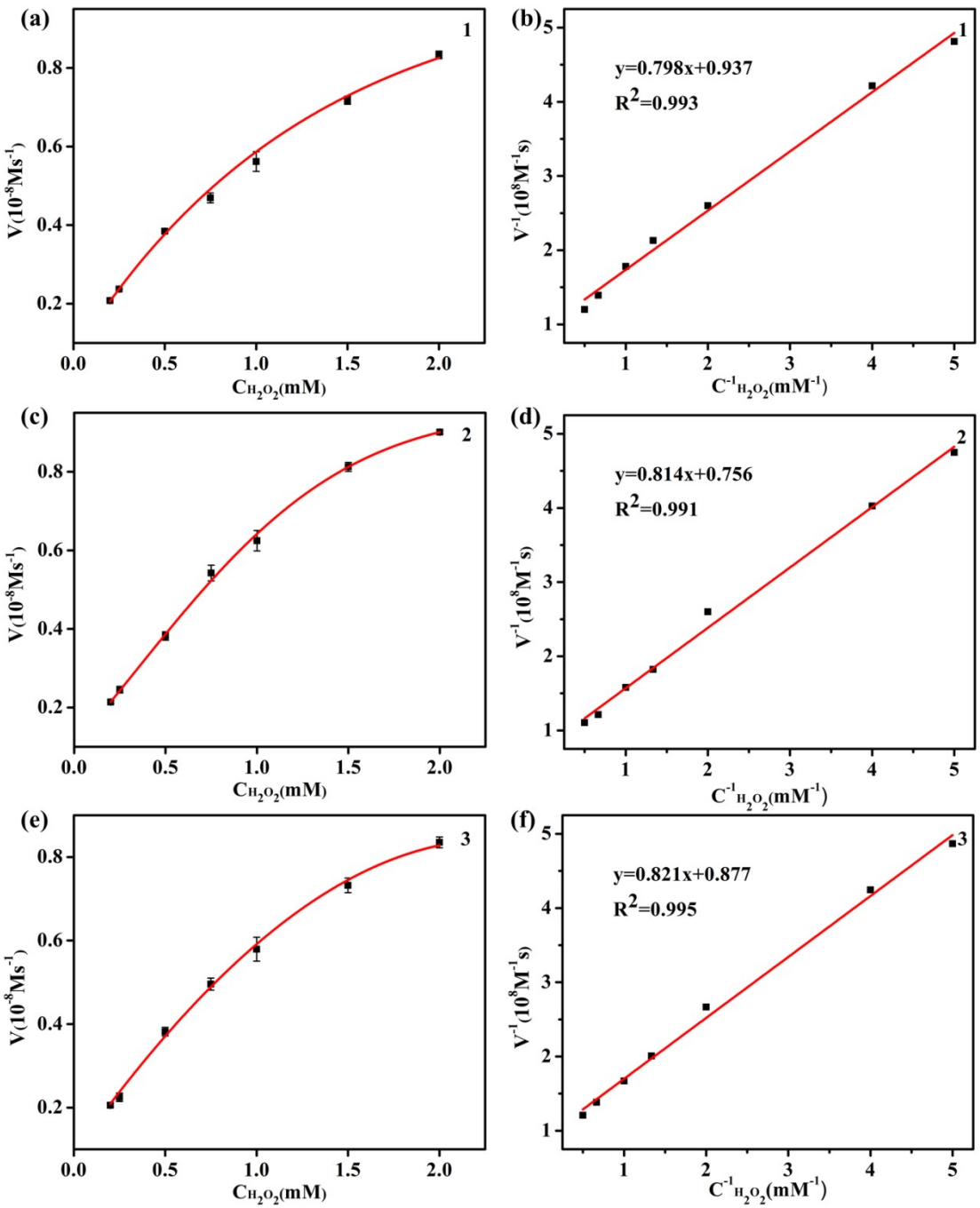

Fig. S11 Kinetic data obtained by varying H_2O_2 concentrations while keeping the concentration of ABTS constant (0.5 mmol L^{-1}), for **1** (a), for **2** (c), for **3** (e) and the Lineweaver-Burk plots of the double reciprocal of the Michaelis-Menten equation for **1** (b), for **2** (d), for **3** (f).

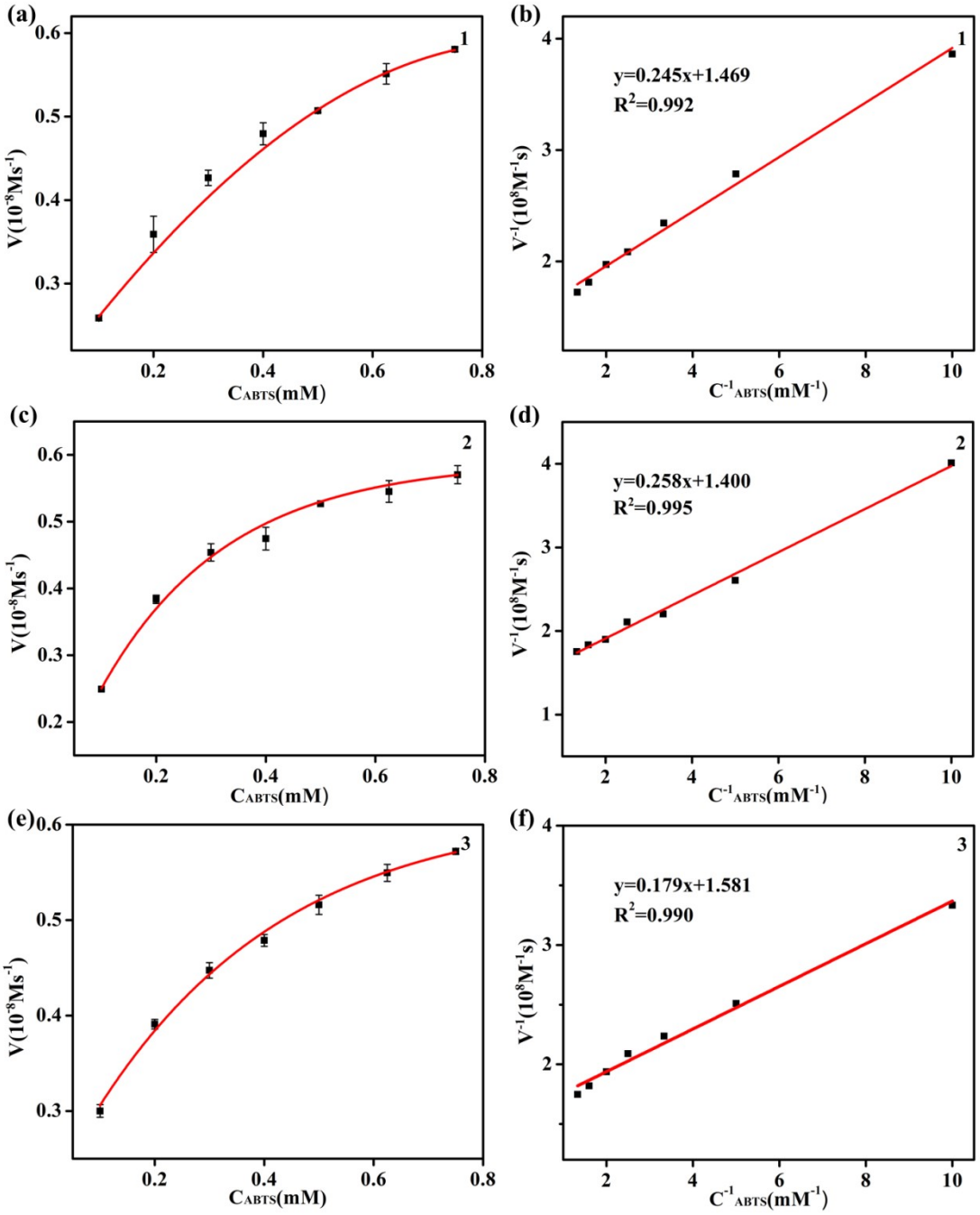

Fig. S12 Kinetic data obtained by varying ABTS concentrations while keeping the concentration of H_2O_2 constant (0.5 mmol L^{-1}) for **1** (a), for **2** (c), for **3** (e) and the Lineweaver-Burk plots of the double reciprocal of the Michaelis-Menten equation for **1** (b), for **2** (d) and for **3** (f).

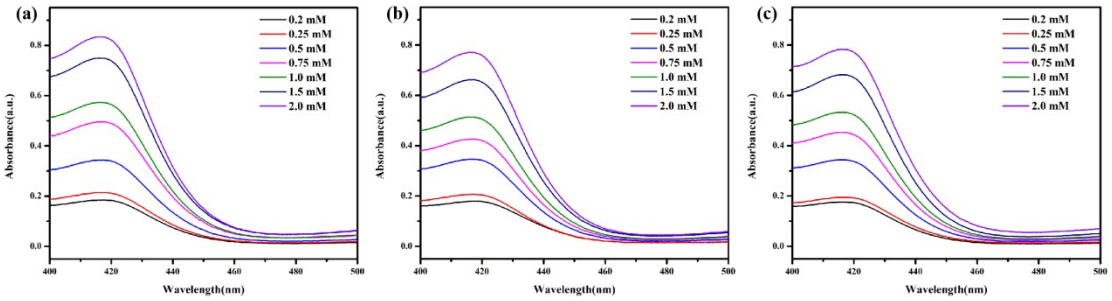

Fig. S13 UV-vis absorbance spectra of kinetic data obtained by varying H_2O_2 concentrations while keeping the concentration of ABTS constant (0.5 mmol L^{-1}), for **1** (a), for **2** (b), for **3** (c).

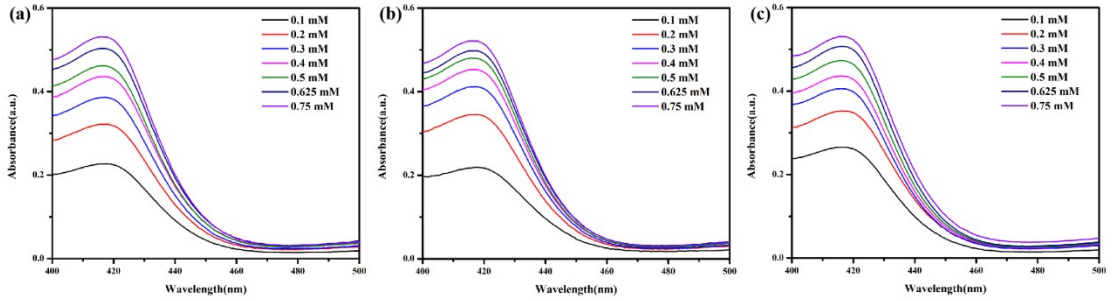

Fig. S14 UV-vis absorbance spectra of kinetic data obtained by varying ABTS concentrations while keeping the concentration of H_2O_2 constant (0.5 mmol L^{-1}), for **1** (a), for **2** (b), for **3** (c).

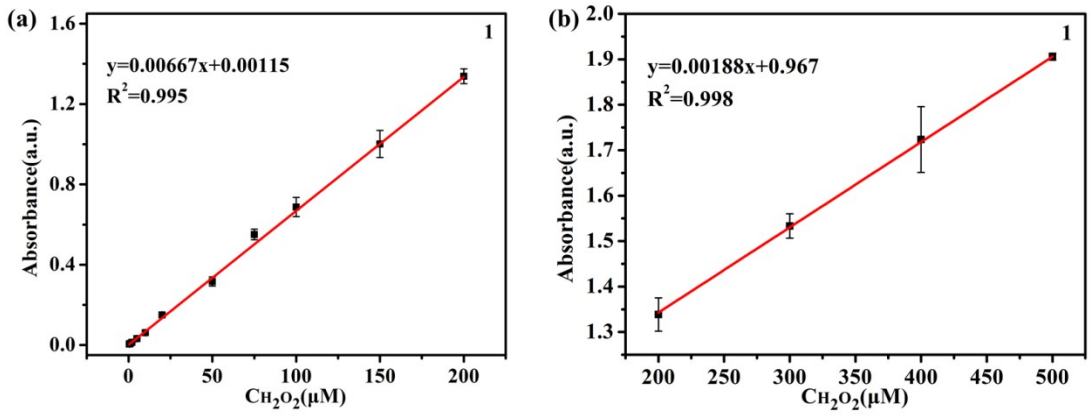

Fig. S15 The corresponding linear calibration plots for H_2O_2 detection of **1** with linear ranges of 0.5 to 200 μM (a), 200 to 500 μM (b).

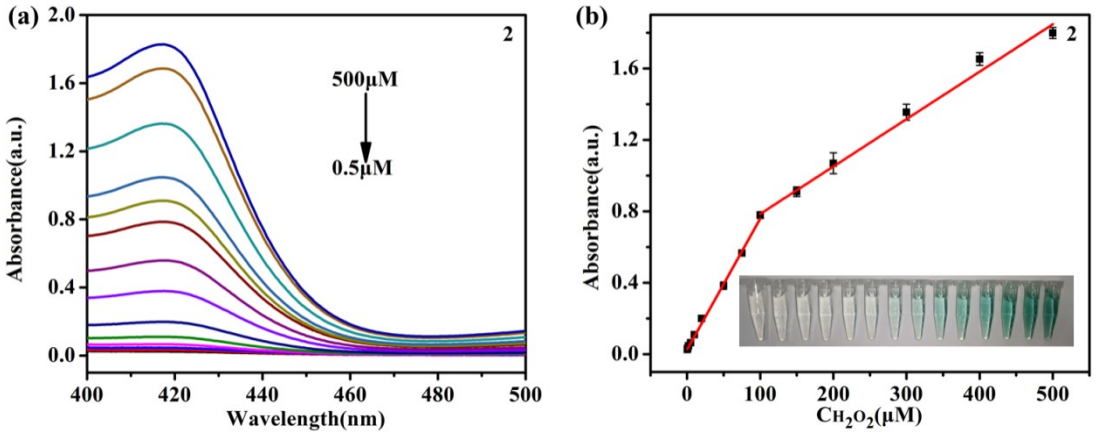

Fig. S16 (a) UV-vis absorbance spectra of ABTS for **2** at varying H_2O_2 concentrations (0.5, 1, 2, 5, 10, 20, 50, 75, 100, 150, 200, 300, 400, 500 μM). (b) The corresponding linear calibration plots for H_2O_2 detection.

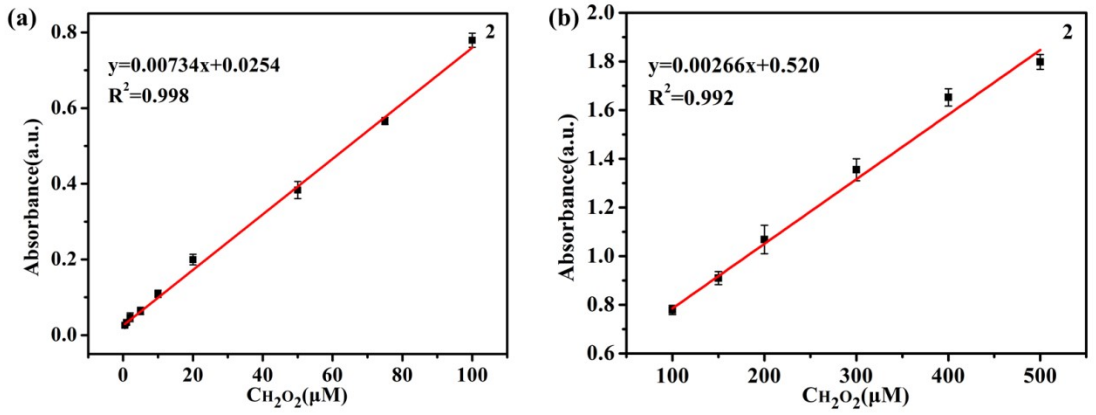

Fig. S17 The corresponding linear calibration plots for H_2O_2 detection of **2** with linear ranges of 0.5 to 100 μM (a), 100 to 500 μM (b).

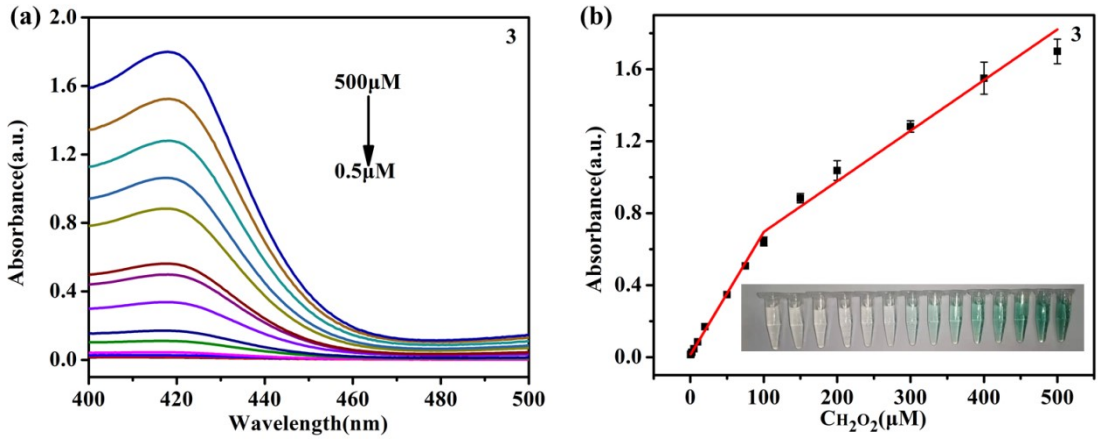

Fig. S18 (a) UV-vis absorbance spectra of ABTS for **3** at varying H_2O_2 concentrations (0.5, 1, 2, 5, 10, 20, 50, 75, 100, 150, 200, 300, 400, 500 μM). (b) The corresponding linear calibration plots for H_2O_2 detection.

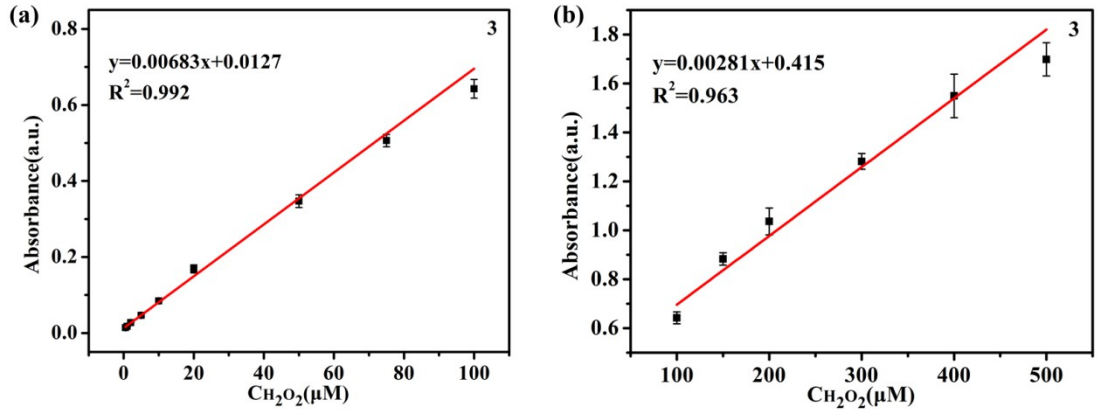

Fig. S19 The corresponding linear calibration plots for H_2O_2 detection of **3** with linear ranges of 0.5 to 100 μM (a), 100 to 500 μM (b).

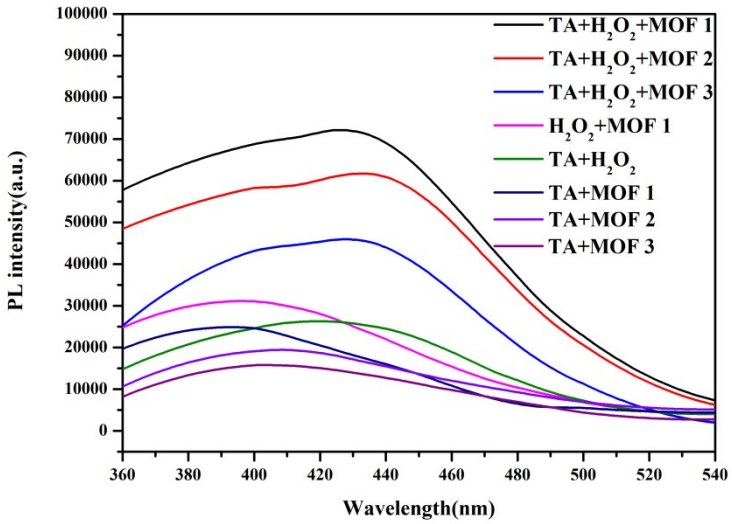

Fig. S20 Investigation the effect of different system on hydroxyl radical generation when terephthalic acid was used as a fluorescent probe.

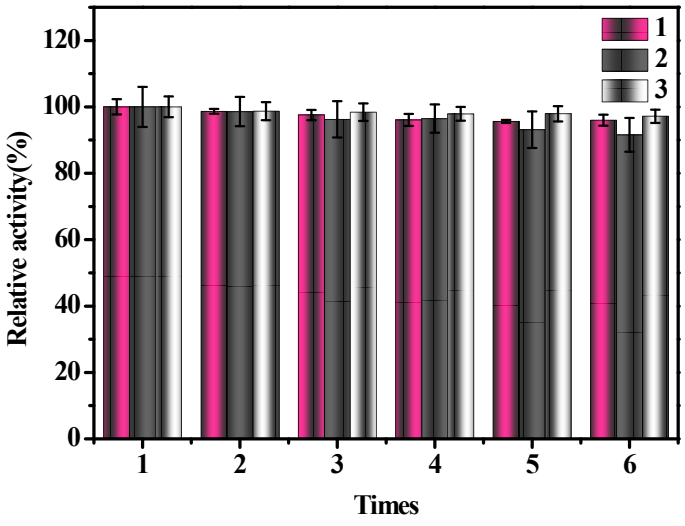

Fig. S21 Relative peroxidase activity of MOFs **1-3** after recycling six times.

Fig. S22 Photographs of selectivity of MOFs **1-3** for H_2O_2. From left to right: isopropyl alcohol (IPA), ethanol (EA), acetone(AC), tetrahydrofuran (THF), ethyl acetate (EAC), DMF, NaCl, KCl, aspartic acid (Asp), glucose (Glu), ascorbic acid (AA), citric acid (CA), salicylic acid (SA) and H_2O_2.

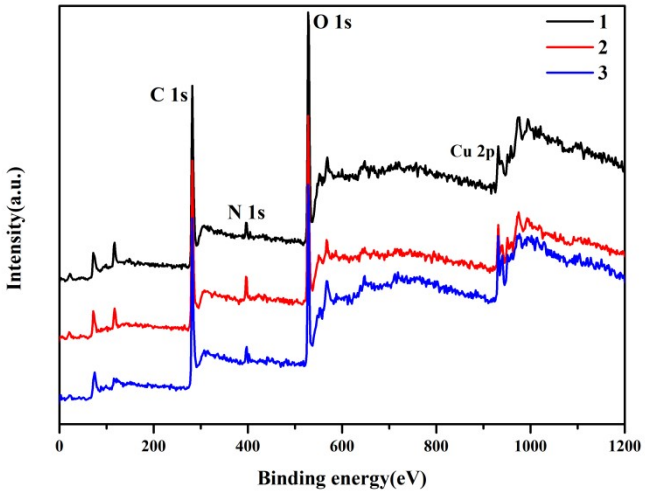

Fig. S23 The XPS spectra of MOFs **1-3**.

Table S1 Crystal and structure refinement data for MOFs 1-3

MOFs	**1**	**2**	**3**
chemical formula	$C_{59}H_{45}Cu_6N_5O_{32}$	$C_{52}H_{30}Cu_3N_6O_{13}$	$C_{56}H_{42}Cu_8N_5O_{38}$
fw	1717.24	1137.44	1901.334
cryst system	triclinic	triclinic	monoclinic
space grow	*P*-1	*P*-1	*C*2/*c*
a/Å	8.4291(15)	9.2608(3)	27.4616(7)
b/Å	16.414(3)	10.6337(4)	23.3296(6)
c/Å	16.973(3)	13.1879(5)	14.1872(4)
α/deg	72.135(7)	82.385(1)	90
β/deg	80.514(7)	85.159(1)	105.775(1)
γ/deg	89.314(9)	70.816(1)	90
V/ Å^3	2202.7(7)	1214.6(1)	8747.0(4)
T/K	170	296	289
Z	1	1	4
D_c/g cm^{-3}	1.295	1.655	1.711
μ/mm^{-1}	1.495	1.372	3.073
F(000)	864.0	615.0	4576
index ranges	-10≤h≤10 -21≤k≤21 -22≤l≤21	-12≤h≤12 -13≤k≤13 -17≤l≤17	-33≤h≤33 -28≤h≤28 -16≤h≤17
R_{int}	0.1044	0.0707	0.0502
GOF on F^2	1.081	1.039	1.054
$R_1[I>2\sigma(I)]$	0.0499	0.0367	0.0377
$wR_2[I>2\sigma(I)]$	0.1451	0.1008	0.1058
CCDC No.	2129142	2129147	2129156

[a] $R_1 = \Sigma||F_o| - |F_c||/\Sigma|F_o|$. [b] $wR_2 = \Sigma[w(F_o^2 - F_c^2)^2]/\Sigma[w(F_o^2)^2]^{1/2}$

Table S2 Selected bond lengths [Å] and angles [°] for MOFs **1**-**3**

1			
Cu(2)-O(4)	1.946(3)	O(1)- Cu(1)	1.955(3)
Cu(2)-O(10)#1	1.959(3)	Cu(1)-O(5)	1.956(3)
Cu(2)-O(2)	1.951(3)	Cu(1)-O(9)#1	1.990(3)
Cu(2)-O(11)#1	1.956(3)	Cu(1)-O(12)#1	1.955(3)
Cu(2)-O(3)	2.146(4)	Cu(3)-O(14)#2	1.971(3)
Cu(3)-O(7)	1.960(3)	Cu(3)-N(2)#3	2.034(3)
Cu(3)-N(1)#4	2.032(3)	Cu(3)-O(6)	2.323(4)
O(4)-Cu(2)-O(10)#1	88.24(14)	O(4)-Cu(2)-O(2)	91.21(14)
O(4)-Cu(2)-O(3)	99.08(16)	O(10)#1-Cu(2)-O(3)	99.40(15)
O(2)-Cu(2)-O(10)#1	169.06(12)	O(2)-Cu(2)-O(3)	91.48(15)
O(11)#1-Cu(2)-O(4)	166.87(13)	O(11)#1-Cu(2)-O(10)#1	90.11(14)
O(11)#1-Cu(2)-O(2)	87.95(14)	O(11)#1-Cu(2)-O(3)	94.04(16)
O(5)-Cu(1)-O(1)	89.43(13)	O(5)-Cu(1)-O(9)#1	88.69(13)
O(9)#1-Cu(1)-O(1)	166.40(12)	O(12)#1-Cu(1)-O(1)	88.28(14)
O(12)#1-Cu(1)-O(5)	168.57(12)	O(12)#1-Cu(1)-O9)#1	90.91(13)
O(14)#2-Cu(3)-N(2)#3	90.95(12)	O(14)#2-Cu(3)-N(1)#4	88.24(12)
O(14)#2-Cu(3)-O(6)	88.81(17)	O(7)-Cu(3)-O(14)#2	177.20(11)
O(7)-Cu(3)-O(2)#3	91.37(12)	O(7)-Cu(3)-N(1)#4	89.67(12)
O(7)-Cu(3)-O(6)	89.43(17)	N(2)#3-Cu(3)-O(6)	94.84(15)
N(1)#4-Cu(3)-N(2)#3	172.45(13)	N(1)#4-Cu(3)-O(6)	92.64(14)

Symmetry transformations used to generate equivalent atoms:

#1 1+X, +Y, +Z; #2 +X, -1+Y, +Z; #3 1-X, 1-Y, -Z; #4 1-X, 1-Y, 1-Z #5 +X, 1+Y, +Z; #6 -1+X, +Y, +Z

2			
Cu(1)-O(3)#1	1.9354(17)	Cu(1)-O(4)	1.9357(18)
Cu(1)-O(5)#2	2.2741(18)	Cu(1)-N(1)	2.030(2)
Cu(1)-N(3)	2.046(2)	O(6)-Cu(3)#3	1.9665(17)
O(6)-Cu(2)#4	1.9676(18)	O(6)-Cu(2)#3	2.055(2)
N(2)-Cu(3)	2.0182(18)	N(2)-Cu(2)#5	2.118(3)
N(2)-Cu(2)	2.020(2)	O(3)#1-Cu(1)-O(4)	96.90(7)
O(3)#1-Cu(1)-O(5)#2	110.94(7)	O(3)#1-Cu(1)-N(1)	90.24(7)
O(3)#1-Cu(1)-N(3)	163.27(7)	O(4)-Cu(1)-O(5)#2	94.01(7)
O(4)-Cu(1)-N(1)	171.44(7)	O(4)-Cu(1)-N(3)	90.98(7)
N(1)-Cu(1)-O(5)#2	87.79(7)	N(1)-Cu(1)-N(3)	80.92(7)
N(3)-Cu(1)-O(5)#2	83.06(7)	O(6)#5-Cu(3)-O(6)#7	180.0
O(6)#7-Cu(3)-N(2)#6	89.14(7)	O(6)#5-Cu(3)-N(2)#6	90.86(7)
O(6)#5-Cu(3)-N(2)	89.14(7)	N(2)#6-Cu(3)-N(2)	180.0
O(6)#5-Cu(2)-O(6)#7	160.8(3)	O(6)#5-Cu(2)-N(2)	91.46(8)
O(6)#5-Cu(2)-N(2)#6	88.84(9)	O(6)#7-Cu(2)-N(2)#6	84.14(11)
N(2)-Cu(2)-N(2)#6	161.4(31)		

Symmetry transformations used to generate equivalent atoms:

#1 -1+X, +Y, +Z; #2 1-X, 1-Y, 1-Z; #3 +X,1+Y, +Z; #4 1+X, +Y, +Z; #5 1-X,1-Y, 2-Z; #6 X, -1+Y, Z; #7 1-X, -Y, 2-Z

3			
Cu(1)-O(12)	1.9200(18)	O(1)-Cu(12) #1	2.368(2)
Cu(1)-O(19)#2	1.9693(18)	Cu(1)-O(15) #3	1.9959(18)
Cu(1)-O(17) #4	1.9739(18)	Cu(3)-O(10)	1.943(2)
Cu(3)-O(6)	1.945(2)	Cu(3)-N(2)	2.000(2)
Cu(3)-N(3)	1.977(2)	O(9)-Cu(4)#5	1.938(2)
Cu(2)-O(14) #6	1.9699(18)	Cu(2)-O(11)	1.9454(18)
Cu(2)-O(12)	1.8839(18)	Cu(2)-O(16) #4	1.9546(18)
Cu(4)-O(2)	1.955(3)	Cu(4)-O(5)	1.976(2)
Cu(4)-O(3)	2.222(3)	Cu(4)-O(4)	1.948(2)
O(12)-Cu(1)-O(12)#1	84.15(8)	O(12)-Cu(1)-O(19)#2	92.00(8)
O(12)-Cu(1)-O(15)#3	173.23(9)	O(12) -Cu(1)-O(17)#4	92.69(8)
O(19)#2-Cu(1)-O(12)#1	89.58(9)	O(19)#2-Cu(1)-O(15) #3	91.80(8)
O(15)#3-Cu(1)-O(12)#1	90.27(8)	O(17)#4-Cu(1)-O(12)#1	95.21(9)
O(17)#4-Cu(1)-O(19)#2	173.61(10)	O(17)#4-Cu(1)-O(15)#3	83.98(8)
O(10)-Cu(3)-O(6)	172.30(8)	O(10)-Cu(3)-N(2)	90.89(9)
O(10)-Cu(3)-N(3)	93.55(10)	O(6)-Cu(3)-N(2)	91.55(9)
O(6)-Cu(3)-N(3)	87.06(10)	O(11)-Cu(2)-O(14)#6	92.55(8)
O(11)-Cu(2)-O(16)#4	83.69(8)	O(12)-Cu(2)-O(14)#6	88.48(8)
O(12)-Cu(2)-O(11)	178.90(9)	O(12)-Cu(2)-O(16)#4	95.32(8)
O(16)#4-Cu(2)-O(14)#6	174.11(9)	O(9)#5-Cu(4)-O(2)	92.80(11)
O(9)#5-Cu(4)-O(5)	84.80(9)	O(9)#5-Cu(4)-O(3)	92.73(15)
O(9)#5-Cu(4)-O(4)	167.74(13)	O(2)-Cu(4)-O(5)	171.37(15)
O(2)-Cu(4)-O(3)	102.88(17)	O(5)-Cu(4)-O(3)	85.54(11)
O(4)-Cu(4)-O(2)	89.67(12)	O(4)-Cu(4)-O(5)	90.99(10)
O(4)-Cu(4)-O(3)	98.43(15)		

Symmetry transformations used to generate equivalent atoms:

#1 1.5-X, 0.5+Y, 0.5-Z; #2 X, 1-Y, -0.5+Z; #3 +X, +Y,-1+Z; #4 1.5-X, 1.5-Y, -Z; #5 1-X, +Y, 1.5-Z;

#6 1.5-X, 1.5-Y, 1-Z; #7 1-X, Y, 0.5-Z; #8 +X,+Y,1+Z; #9 +X,1-Y, 0.5+Z; #10 1.5-X, -0.5+Y, 0.5-Z

Table S3 Mild oxidation of cycloalkanes (C6 and C8) in the presence of catalysts **1-3**[a]

		20 ℃			40 ℃			60 ℃		
	hydrocarbon	Cyclic alcohol	Cyclic ketone	total[c]	Cyclic alcohol	Cyclic ketone	total[c]	Cyclic alcohol	Cyclic ketone	total[c]
1	cyclohexane	0.05	0.27	0.31	8.04	6.21	14.25	11.08	8.63	19.71
	cyclooctane	trace	0.89	0.89	1.07	5.25	6.32	1.14	4.33	5.47
2	cyclohexane	trace	0.66	0.66	10.07	11.16	21.23	13.06	12.25	25.31
	cyclooctane	trace	1.05	1.05	1.90	7.09	8.99	3.08	7.26	10.34
3	cyclohexane	trace	1.23	1.23	11.21	7.09	18.30	14.72	11.24	25.96
	cyclooctane	trace	0.21	0.21	3.12	8.53	11.65	2.04	7.04	9.08

[a]Conditions of the reactions: cycloalkane, 1 mmol; catalysts **1-3**, 10 μmol; H_2O_2, 5 mmol; MeCN, 2.5 mL; time, 6 h. [b]Yields were calculated as (moles of product per mole of cycloalkane) × 100%；typically determined by GC after the treatment with PPh_3. [c]Sum of the alcohol and ketone yields.

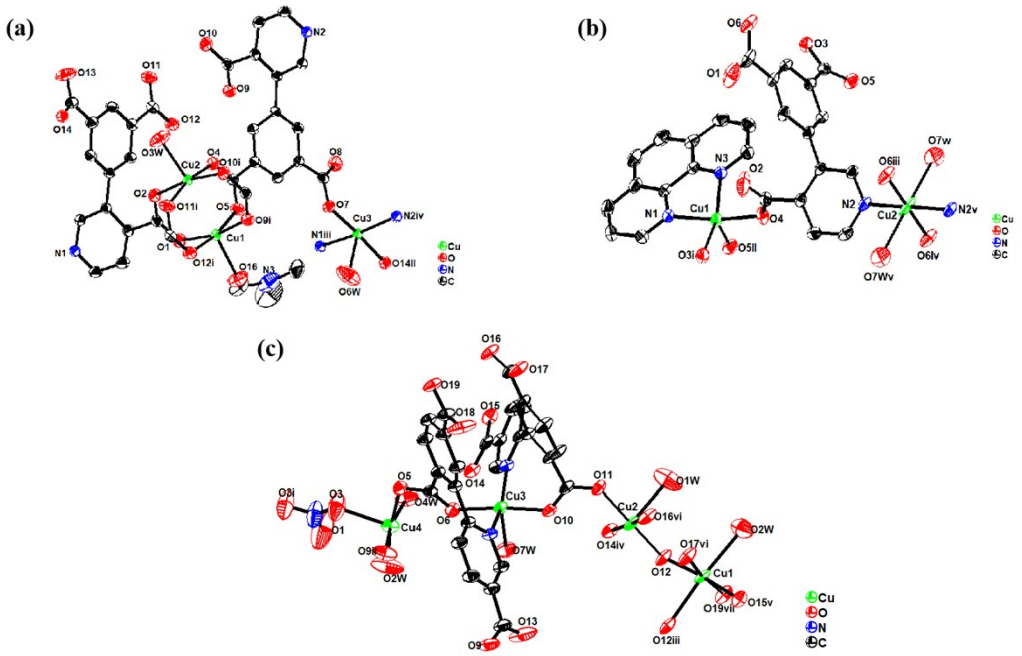

Fig. S24 The ORTEP diagrams of MOF **1** (a), **2** (b), **3** (c) (probability level 50%).Symmetry equivalent positions are (i) 1+x, y, z; (ii) x, -1+y, z, (iii) 1-x, 1-y, 1-z; (iv) 1-x, 1-y, -z for MOF **1**; (i) -1+x, y, z; (ii) 1-x, 1-y, 1-z, (iii) 1-x, 1-y, 2-z; (iv) x, -1+y, z for MOF **2**; (i) 1-x, y,1.5-z; (ii) 1-x, y, 0.5-z, (iii) 1.5-x, 1.5-y, -z; (iv) 1.5-x, 1-y, 1-z, (v) x, y, -1+z; (vi) x, 1-y, -0.5+z for MOF **3**.